Validating Large-Deformation Diffeomorphic Metric Matching in Hippocampus

Lei Wang[1], M. Faisal Beg[2], John T. Ratnanather[3], John G. Csernansky[1], Michael I. Miller[3]
[1]Department of Psychiatry, Washington University School of Medicine, St. Louis, MO, [2]School of Engineering Science, Simon Fraser University, Burnaby, BC, Canada, [3]Center for Imaging Science, Johns Hopkins University, Baltimore, MD 21218
Supported by P50 MH71616 56429, R01 MH 60883, R01 MH 56584, P01 AG03991, P50 AG05681, AG 05684, NSERC 31-611387, P41-RR15241, R01-MH064838

Introduction

We compare the results of two different implementations of large-deformation diffeomorphic image mapping.

Computational Anatomy and Large-Deformation Diffeomorphic Image Matching

In Computational Anatomy, the anatomic model is a quadruple $(\Omega, \mathcal{G}, \mathcal{I}, \mathcal{P})$, consisting of

$\Omega \subset \mathbb{R}^d$	the template coordinate space
$\mathcal{G}$	a subset of diffeomorphisms on Ω
$\mathcal{I}$	the orbit of anatomical imagery under $\mathcal{P}$
$\mathcal{P}$	the family of probability laws of anatomical variation on $\mathcal{I}$ [1].

The diffeomorphisms are modeled as evolution in time, or a flow g_t, $t\in[0,1]$ with an associated velocity vector field $v_t \in \mathcal{V}$, $t\in[0,1]$ that controls the evolution:

$$\mathcal{V} = \left\{ v_t : \Omega \to \mathbb{R}^d, \|v_t\|_{\mathcal{V}}^2 < \infty, t\in[0,1] \right\}.$$

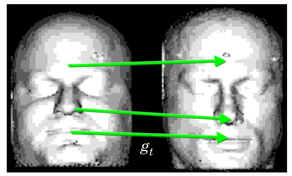

The forward and inverse maps are given by ordinary differential equations (ODE):

$$\frac{\partial g_t}{\partial t} = v_t(g_t) \text{ and } \frac{\partial g_t^{-1}}{\partial t} = -D(g_t^{-1})\, v_t,\ t\in[0,1], \text{on } \Omega$$

$g_0 = g_0^{-1} = \mathrm{id}$	the identity map
Df the $d\times d$	Jacobian matrix
$v_t \in \mathcal{V}$	the velocity vector field

Smoothness of the velocity vector field ensures that the set of solutions to the ODEs is the subgroup of diffeomorphisms (details given in [2, 3]):

$$\mathcal{G} = \left\{ g_1 : \frac{\partial g_t}{\partial t} = v_t(g_t), t\in[0,1], v\in\mathcal{V} \right\}.$$

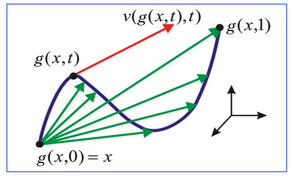

Given observable anatomical images	$I_0, I_1 \in \mathcal{I}$
the solution to the variational problem	$\min_{v_t} \int_0^1 \|v_t\|_{\mathcal{V}}^2 dt + \left\| I_1 - I_0(g_1^{-1}) \right\|^2$
gives rise to the optimal changes of coordinates	$\hat{g}_1$
such that	$I_0(\hat{g}_1^{-1}) \approx I_1$

Globally-Optimal Algorithm Implementation and Metrics for Homogeneous Image Space

This is the large-deformation diffeomorphic metric mapping (LDDMM) solution developed by Beg et al [4]. LDDMM is similar to the large-deformation diffeomorphic image mapping put forward in [5] by Christensen et al (below), but in contrast to [5] the arc length of the geodesic

$$\inf \int_0^1 \|v_t\|_{\mathcal{V}} dt$$

connecting the two images under mapping defines a metric distance between two images on $\mathcal{I}$.

Locally-Optimal ("Greedy") Algorithm Implementation

The Christensen algorithm discretizes the space-time continuum

$$\Omega \times [0,1]$$

thereby turns the solution of ODE into a sequence of time-indexed optimizations solving for locally optimal velocity at each time and then forward integrating the solution. This locally-in-time "greedy" algorithm does not give the image orbit a metric distance.

Methods

Subjects and Scans

- 5 matched pairs of schizophrenia and young control subjects
- 5 matched pairs of very mild dementia of the Alzheimer type (DAT) and elderly control subjects
- Magnetom SP-4000 1.5-Tesla Siemens imaging system with standard head coil
- 3D MPRAGE sequence

  (TR = 10 ms, TE = 4 ms, flip angle = 30°, 1.25 mm section thickness, 128 slices, 256-mm field of view, matrix 256 × 256, number of acquisitions = 1, scanning time = 5.6 min @ 1 × 1 × 1.25 mm^3/voxel)

Step 1. Small-Deformation Landmark Matching

Landmarks are laid out according to AC–PC (global) and hippocampal (local) orientations. The initial alignment of the template and target regions of interest are based on these landmarks [6].

Global landmarks (AC – PC orientation)

+

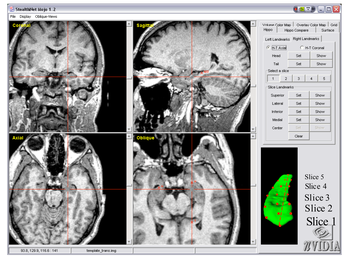

Local landmarks (hippocampal orientation)

Step 2. Large-Deformation Image Matching

Intensity-based diffeomorphic mapping is performed on the regions of interest via either algorithm.

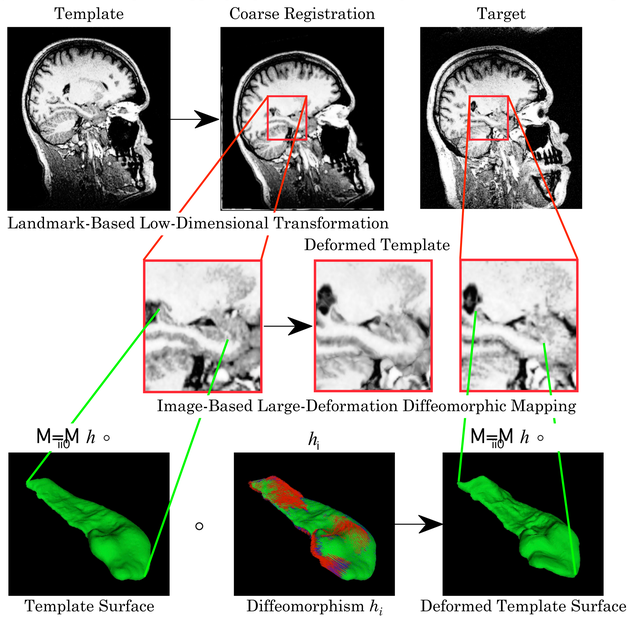

Results

Template subvolume

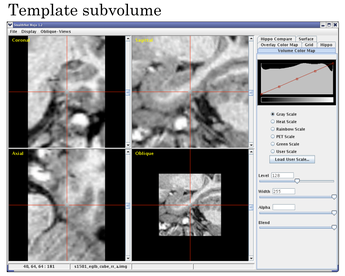

Target subvolume

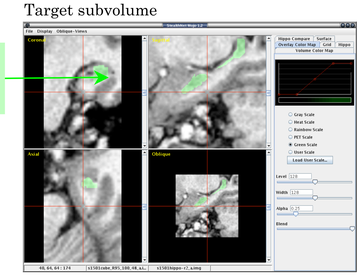

$\mathcal{R}$: reference (manual) segmentation gray matter

Deformed Template – "Greedy" algorithm

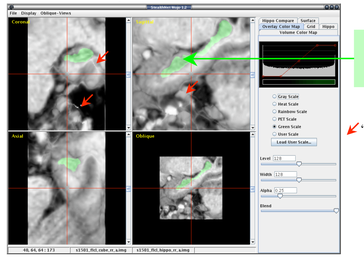

"Streaking"

No "Streaking"

Deformed Template – LDDMM

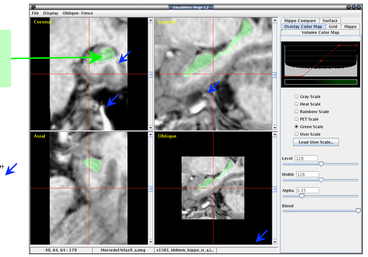

$\mathcal{A}$: automated segmentation gray matter

Accuracy Assessments

$\mathcal{R}$: reference (manual) segmentation with M tissue types (eg, gray matter), with posteriori probabilities $p^{\mathcal{R}}(h_n \mid I_n)$ 0 or 1

$\mathcal{A}$: automated segmentation with the same tissue types with posteriori probabilities $p^{\mathcal{A}}(h_n \mid I_n)$

$$\%\ \text{voxel overlap} = \frac{\text{Vox}_{\mathcal{R}} \cap \text{Vox}_{\mathcal{A}}}{\text{Vox}_{\mathcal{R}}} \times 100$$

$$L_1\ \text{error} = \frac{1}{2N} \sum_{n=1}^{N} \sum_{i=1}^{M} \left| p^{\mathcal{A}}(h_n = H_i \mid I_n) - p^{\mathcal{R}}(h_n = H_i \mid I_n) \right|$$

Study	Algorithm	% Voxel Overlap	L_1 error
Schizophrenia (n=5) Control (n=5) (MR data taken from [7])	Christensen	79.45 (±2.97)	0.230 (±0.025)
	Beg (LDDMM)	79.56 (±2.72)	0.226 (±0.026)
DAT (n=5) Control (n=5) (MR data taken from [8])	Christensen	80.62 (±5.52)	0.220 (±0.048)
	Beg (LDDMM)	78.54 (±5.80)	0.201 (±0.026)

Conclusion

The globally-optimal solution of the Beg (LDDMM) algorithm which gives rise to a metric distance between biological shapes is no less accurate than the locally-optimal "greedy" solution of the Christensen algorithm which does not define a metric distance.

References

1. M. I. Miller, "Computational anatomy: shape, growth, and atrophy comparison via diffeomorphisms," Neuroimage, vol. 23 Suppl 1, pp. S19-33, 2004.
2. P. Dupuis, U. Grenander, and M. I. Miller, "Variational problems on flows of diffeomorphisms for image matching," Quarterly of Applied Mathematics, vol. LVI, pp. 587-600, 1998.
3. A. Trouve, "An infinite dimensional group approach for physics based models in pattern recognition," LMENS/DIAM, URA 762, Ecole Normale Superieure, Paris, Technical Report 1995.
4. M. F. Beg, M. I. Miller, A. Trouve, and L. Younes, "Computing Large Deformation Metric Mappings via Geodesic Flows of Diffeomorphisms," International Journal of Computer Vision, vol. 61, pp. 139, 2005.
5. G. E. Christensen, R. D. Rabbitt, and M. I. Miller, "Deformable templates using large deformation kinematics," IEEE Transactions on Image Processing, vol. 5, pp. 1-13, 1996.
6. S. Joshi, M. I. Miller, and U. Grenander, "On the geometry and shape of brain sub-manifolds.," Int J Pattern Recog Artificial Intell (Special Issue), vol. 11, pp. 1317-1343, 1997.
7. J. G. Csernansky, L. Wang, S. Joshi, J. P. Miller, M. Gado, D. Kido, D. McKeel, J. C. Morris, and M. I. Miller, "Early DAT is distinguished from aging by high-dimensional mapping of the hippocampus.," Neurology, vol. 55, pp. 1636-43, 2000.
8. J. W. Haller, A. Banerjee, G. E. Christensen, M. Gado, S. Joshi, M. I. Miller, Y. Sheline, M. W. Vannier, and J. G. Csernansky, "Three-dimensional hippocampal MR morphometry with high-dimensional transformation of a neuroanatomic atlas," Radiology, vol. 202, pp. 504-10, 1997.